THE HONG KONG INSTITUTION OF ENGINEERS

Wireless inchworm using small tapped-inductor converter

Hayata Takashima, Akihiro Torii, Kae Doki and Suguru Mototani
Department of Electrical and Electronics Engineering, Aichi Institute of Technology, Japan

ABSTRACT

This paper describes a wireless inchworm with a small battery and a control circuit which eliminate the effect of wiring tension. The inchworm consists of piezoelectric actuators and electromagnets. A converter with a high boost ratio is required to boost the voltage from the battery to the maximum applied voltage of the piezoelectric actuators. The boost converter with a tapped inductor achieves a high boost ratio of approximately 16.7. The input and output voltage for the resistive and capacitive load are measured experimentally. The wireless inchworm loads an onboard microprocessor which operates the electromagnets and piezoelectric actuators. The operation of the wireless inchworm powered by a small battery is described, and the linear displacement is measured. The experimental results show that the small battery can drive the wireless inchworm.

KEYWORDS Inchworm; tapped-inductor boost converter; piezoelectric actuator; electromagnet; micro motion
CONTACT Torii Akihiro torii@aitech.ac.jp
Received 27 February 2024

1. Introduction

The miniaturisation and improvement of various products are rapidly progressing. Small components are highly integrated. However, these components are manufactured by massive and heavy systems or machines such as machine tools and industrial machinery. Compact production systems such as "microfactory" and "desktop factory" have been proposed. The advantages of the compact production systems are energy, space, resources, vibration, noise, cost, etc. (Montes and Olleros, 2020; Okazaki, 2010; Okazaki et al., 2004).

Inchworm is a biomimetic technology that combines a clamping mechanism and a movement mechanism to mimic the action of an inchworm. These mechanisms repeat their movements synchronously, enabling movement in the precision range and a wide operating range, comparatively. Due to these features, linear actuators (Ma et al., 2023; Sun et al., 2022), rotary actuators (Wang et al., 2018; Wang et al., 2020), walker-push types (Hua et al., 2014; Ma et al., 2022) and micro-robot (Smith et al., 2022; Tanabe et al., 2023) have been proposed in the aerospace, medical and industrial sectors.

Multi-degree-of-freedom inchworm actuators were developed for the application of positioning or motion devices (Torii et al., 2012; Torii et al., 2018). The inchworms are composed of piezoelectric actuators (piezos) and electromagnets. The inchworm has an unlimited working area according to the inchworm principle. However, the motion of the inchworm is disturbed by electrical power supply cables. Furthermore, wiring tension forces the inchworm to move on a different trajectory from the target one. Therefore, it was attempted to realise wireless inchworm by means of wireless power transfer (WPT) (Kuroda et al., 2021; Otake et al., 2021). The inchworms using the piezos and electromagnets cause impedance fluctuations, and are currently in the simulation stage. There is also the possibility that the inchworms using electromagnets and WPT may not be compatible.

Dry cell batteries are compact voltage sources which can supply power to the inchworms. The voltage is at most 9 V, and a boost converter with a high boost ratio is required for the drive of the piezo. A high step-up ratio boost converter boosts the voltage from the dry cell battery level to the piezo drive level. The high boost ratio is realised by a tapped-inductor boost converter. The tapped inductor is used in a buck, boost, and buck-boost DC/DC converter (Si et al., 2014). The boost ratio of the tapped-inductor converter is larger than that of the conventional converter. Tapped-inductor boost converters are used in automotive converters (Bez et al., 2018) and solar panel systems (Bentouati et al., 2021) due to their high boost ratio.

This paper proposes a simple wireless inchworm using a tapped-inductor boost converter and a battery. A prototype is manufactured. The prototype experimentally demonstrates the feasibility of the inchworm with the converter and battery. The operation of the inchworm is described in detail in Section 2. The topology and operation of the tapped-inductor DC/DC converter is experimentally described in Section 3. The experiments and results of the wireless inchworm using the fabricated tapped-inductor boost converter and batteries is described in Section 4.

2. Inchworm

Figure 1 shows the developed inchworm (Torii et al., 2012). The inchworm consists of three stacked-type piezoelectric actuators (piezos) for obtaining precision displacement and three electromagnets for clamping.

An equilateral triangle is formed with three piezos, and electromagnets are attached to the vertices of the triangle, respectively. The piezos (NEC-tokin, AE0505D16DF, 0.18 µF at 1 kHz, 1 Vrms) statically extend 17.4 µm by the applied voltage of 150 VDC. The inchworm repeats the deformation of the piezos and excitation of the electromagnets.

Figure 2 shows the operating principle diagram of inchworm linear motion. The position of the inchworm is defined as the position of electromagnet A. The control signals that realise the operation of Figure 2 are shown in Figure 3. Figure 2 and 3 are divided into four intervals.

(a) Electromagnet B and electromagnet C are excited, and electromagnet A is not excited;
(b) Piezo b and piezo c extend and move the non-excited electromagnet A, and electromagnet A moves in the y-direction;
(c) Piezo b and piezo c remain in an extended state. Electromagnet A is excited and holds the position. Electromagnet B and electromagnet C are switched to a non-excited state; and
(d) Non-excited electromagnet B and electromagnet C move by shrinking piezo b and piezo c.

By synchronous sequence control of the piezo and electromagnets as shown in Figure 2 and 3, the inchworm moves in a linear motion in the y-direction. Two piezos (piezo b and piezo c) are driven by this principle. The displacement of the inchworm per one control cycle is proportional to the deformation of the piezo.

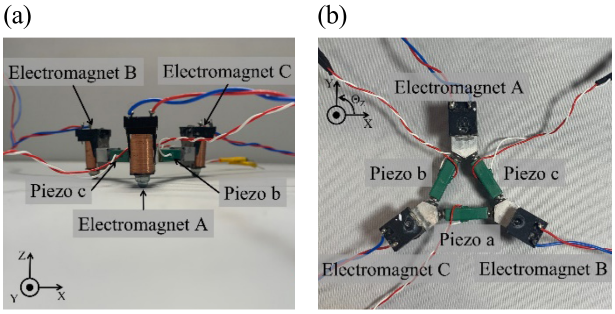

Figure 1. Photograph of inchworm in (a) side view; and (b) top view.

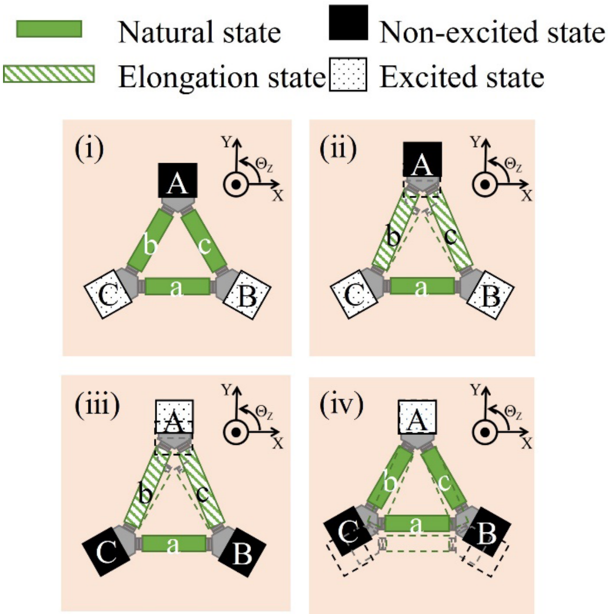

Figure 2. Operating principle of inchworm linear motion.

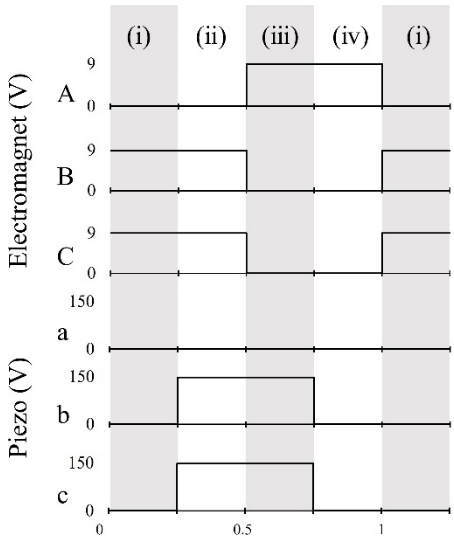

Figure 3. Control signals for linear motion of inchworm.

3. Tapped-inductor boost converter

3.1. Structure of the boost converter

A tapped-inductor boost converter can be easily realised by adding an intermediate tap to the inductor of a conventional boost converter (Liu et al., 2018). Figure 4 shows a tapped-inductor boost converter circuit. An inductor L_2 is added to a conventional boost converter. Two inductors L_1 and L_2 are magnetically and additively connected in series. The tapped inductor has two inductors with two different wires wound on a single core. The turn ratio of the tapped inductor provides an additional voltage boost of the output. It is possible to increase the boost ratio while the size of the converter is maintained. The basic principle of operation of the tapped-inductor boost converter is the same as that of a conventional boost converter. Energy is stored in L_1 during the on-period of switch Q, and the energy is transferred to the load during the off-period of switch Q (Poddar, 2021). The output voltage V_o of the tapped-inductor converter is expressed in Equation (1) (Poddar, 2021), and that of the conventional converter is expressed in Equation (2).

$$V_o = \frac{1 + \frac{n_2}{n_1} d}{1 - d} V_i \, , \tag{1}$$

$$V_o = \frac{1}{1 - d} V_i \, . \tag{2}$$

The voltage V_i denotes the input voltage, and the turn numbers n_1 and n_2 denote the turns of the primary and secondary coil of the tapped inductor, respectively. The letter d denotes the duty ratio of the on-period of switch Q of the drive period. From Equations (1) and (2), the output voltage of the tapped-inductor converter is larger than that of the conventional converter, although the space occupied by the converter is not increased.

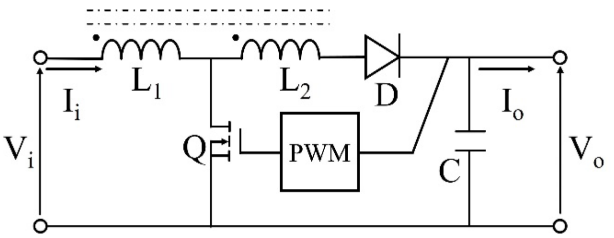

Figure 4. Tapped-inductor boost converter circuit diagram.

3.2. Characteristics of the boost converter

The components and parameters of the fabricated tapped-inductor boost converter are summarised in Table 1. In this experiment, a 9 V battery is used as a voltage source. The fabricated boost converter outputs a stable voltage by feeding back the output voltage with a controller. The boost ratio equals 16.7 which is designed from the maximum voltage of the piezo of 150 V. The operating frequency of switch Q is 25.6 kHz, and the duty ratio is 78.3%. The piezo driven by DC voltage is represented by a capacitor and a resistor connected in parallel, and the resistance is quite large. Therefore, the load resistance used in the resistive load equals 15 kΩ. The internal resistance of the inductor has a significant impact on the boost ratio. The theoretical ratio calculated by Equation (1) equals 31.7 which is twice 16.7. The internal resistance reduces the boost ratio of the converter.

Figure 5 shows (a) input voltage; (b) input current; (c) output voltage; and (d) output current when a 15 kΩ load resistor is connected. As shown in Figure 5(b), the converter is operated in a discontinuous conduction mode (DCM) due to the high load resistance. The output voltage, 150 V, is obtained in Figure 5(c). The efficiency is 59.0%. The transferred power is so small that the fixed loss of the PWM circuit is relatively large. Figure 6 shows (a) input voltage; (b) input current; (c) output voltage; and (d) output current when the piezo is connected instead of the load resistor. From Figure 6(a) and 6(c), the input and output voltages are stable and similar to those obtained with a resistive load. Figure 6(b) shows the similar behavior of the load resistance. Figure 6(d) shows that the output current is constantly pulsating with current. Piezos are capacitive loads and have low power consumption. The converter operates intermittently, and the output power is also supplied discontinuously, since the power consumption is low.

Table 1. Parameters of boost converter.

Tapped inductor	n1:n2=10:75, L1:L2=6.1 μH:293.0 μH
C	10 μF
D	Fast recovery diode, ERA32-02
Q	nMOSFET, TK15A20D
Controller	MC34063A

4. Wireless inchworm

4.1. Design

The inchworm control circuit using the tapped-inductor boost converter was fabricated. The control circuit is shown in Figure 7. The circuit consists of a 9 V battery (CAESEA, 6LR61, 1000 mA, 3.7 Wh, lithium-ion battery) as a voltage source, Arduino nano, electromagnet drive circuit, voltage boost circuit, and piezo drive circuit. An Arduino nano is operated via a three-terminal regulator. Three electromagnets with free-wheeling diodes are directly driven by the battery with serial-connected MOSFETs. The voltage boost circuit boosts the battery voltage to a high voltage appropriate for the piezo drive. Two piezos are connected in parallel and extend and contract simultaneously, since the linear displacement of the inchworm described in Figure 2 and Figure 3 uses two piezos. A 15 kΩ resistor is connected in series with the piezos to prevent short-circuiting of the output current and the boost converter always operates at DCM. The piezos are driven by a parallel-connected MOSFET. These MOSFETs are controlled by the Arduino nano. The wireless inchworm prototype presented in this paper does not adjust the output voltage Vo, although the output voltage can be changed using a PWM circuit in the boost converter.

Figure 8 shows photographs of the wireless inchworm fabricated. The circuit shown in Figure 7 is loaded on

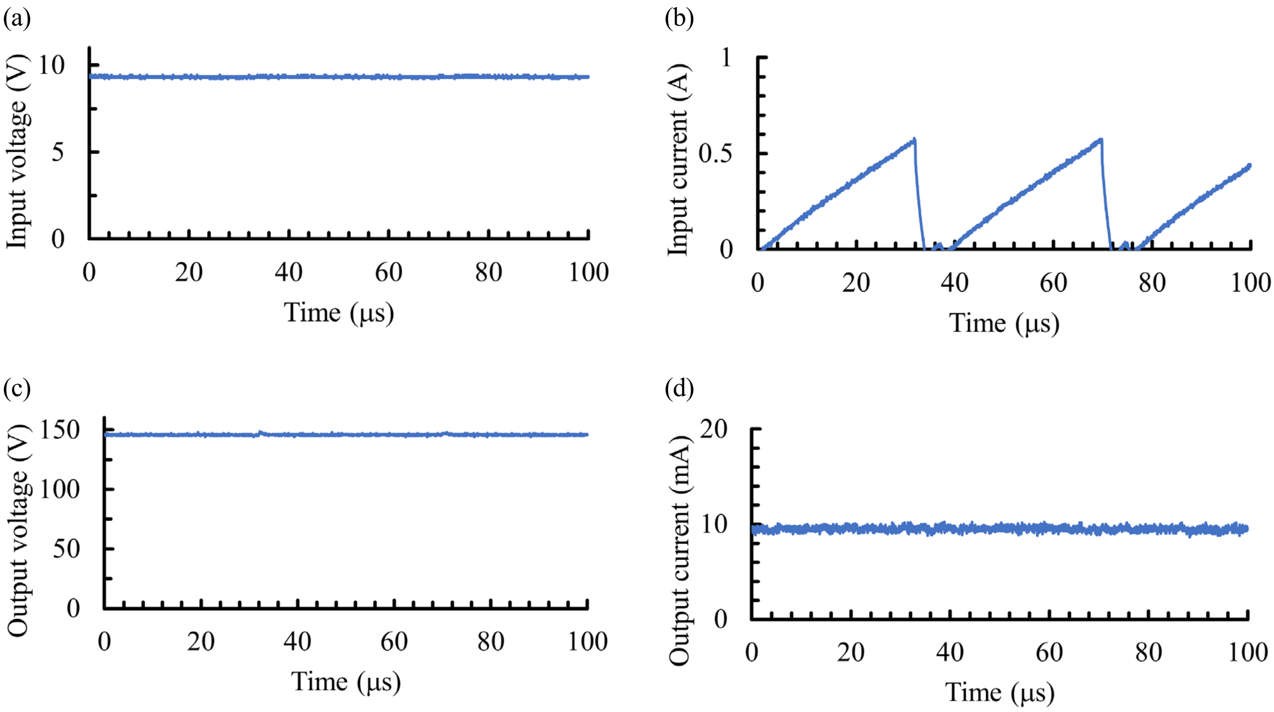

Figure 5. Input/output characteristic of tapped-inductor boost converter with resistor load: (a) input voltage; (b) input current; (c) output voltage; and (d) output current.

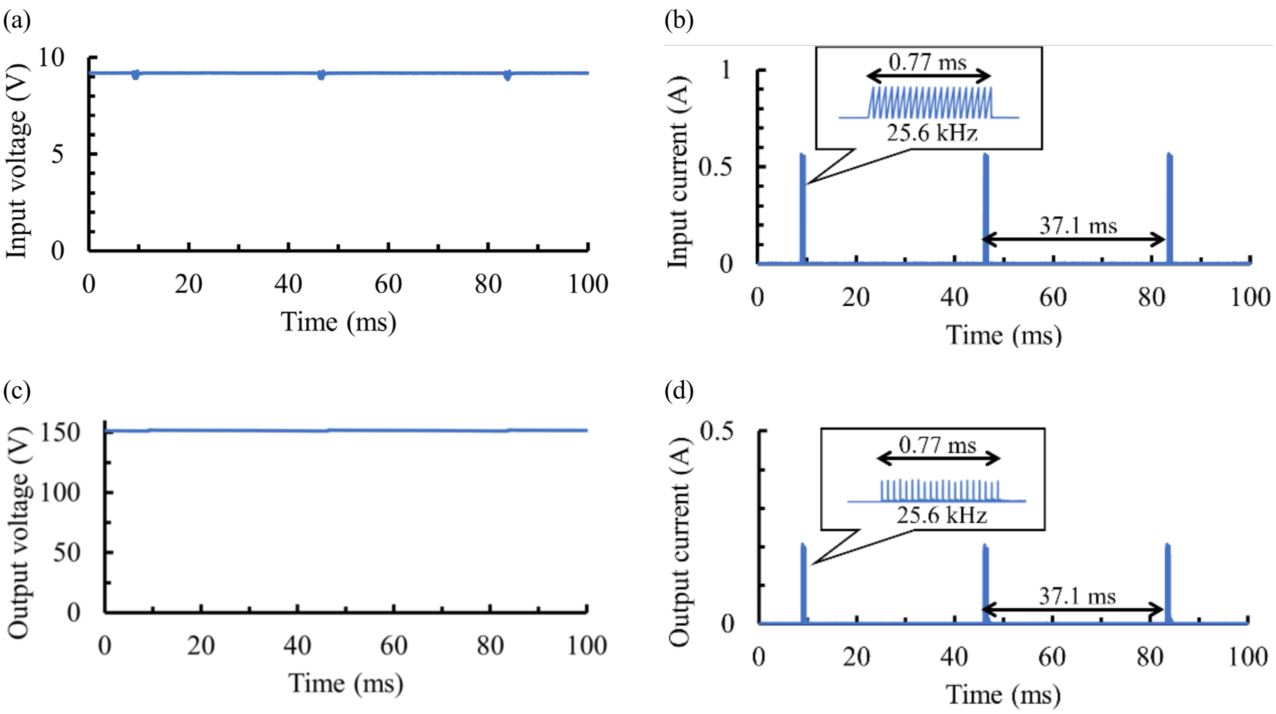

Figure 6. Input/output characteristic of tapped-inductor boost converter with piezo: (a) input voltage; (b) input current; (c) output voltage; and (d) output current.

the inchworm, which weighs 180.3 g and has a height of 6.8 cm. The inchworm moves in a linear direction by using the movement principle shown in Figure 2 with a drive frequency of 1 Hz. The movement of the inchworm is measured by a laser displacement meter (Keyence, LK-G30A).

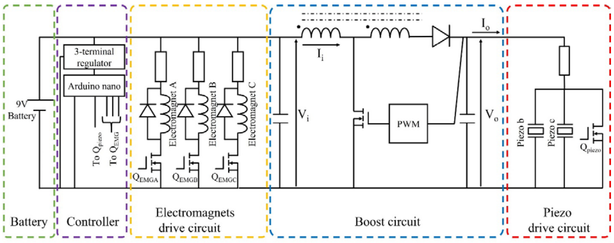

Figure 7. Circuit diagram of wireless inchworm.

(a) (b)

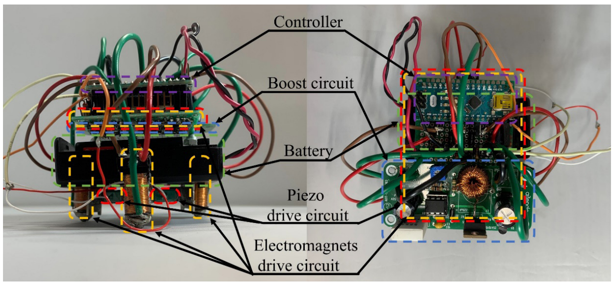

Figure 8. Photographs of wireless inchworm in (a) side view; and (b) top view.

4.2. Operation of the wireless inchworm

Figure 9 shows the input/output characteristic of the tapped-inductor boost converter while the wireless inchworm moves with 1 Hz. The input and output voltage fluctuates in Figure 9(a) and 9(c). The input voltage fluctuates 0.5 V between 8.9 V and 9.4 V, and the output voltage fluctuates 7 V between 150 V and 143 V in conjunction with the switching of the piezos. This voltage fluctuation is caused by the switching of the piezos. Figure 9(b) shows the input current. The input current varies with the drive frequency depending on the charging status of the piezo. The output current shown in Figure 9(d) similarly fluctuates due to the switching of the piezo. The output current decreases as the electric charge of the piezo is charged, and the current stops flowing when the piezo is fully extended. In contrast, during piezo contraction, the current changes quickly due to the discharge of the electric charge to the ground. Therefore, a rush current is generated. However, the current at the output of the boost converter is small, and the discharge of the piezo takes time, which means that the amount of rush current is small and is not considered to be a problem. From Figure 9, the input and output power are 1.3 W and 0.69 W, and therefore the efficiency of the converter is approximately 53.2%. Since the prototype is fabricated with discrete components, the loss is large and the efficiency is low.

The currents of electromagnets A and B and the voltage of piezo b during wireless inchworm operation are shown in Figure 10. A similar current flows in electromagnet C as in electromagnet B, which is connected in parallel, and the voltage in piezo c is similar to that in piezo b. A current of approximately 36 mA, the rated current, flows through the electromagnets, and a voltage of 150 V is applied to the piezo via a boost converter. The electromagnet current increases or decreases with the timing of the switching of the piezo element, which is considered to be an effect of impedance fluctuations caused by the switching of the piezos. However, the fluctuation range is approximately 1 mA, which is not considered to be a problem.

Figure 11 shows an example of the displacement of a conventional inchworm connected with external devices and a fabricated wireless inchworm. The wireless inchworm achieved a linear displacement of 183.3 μm in 20 cycles, with a movement of 9.17 μm per cycle. The conventional wired inchworm achieved a linear displacement of 169.3 μm in 20 cycles, with a movement of 8.47 μm per cycle. The amount of movement improved by 8.3%. Up to cycle 6, both inchworms showed similar amounts of movement, after which the conventional inchworm showed the greater movement up to cycle 13. After that, the conventional inchworm moved less per cycle than the wireless inchworm. In contrast, the wireless inchworm moved with a similar amount of movement throughout the 20 cycles. This is considered a significant effect of the wiring tension on the inchworm and a barrier to expanding its operating range and precision movement. It is also considered that wireless inchworms are one effective solution to these problems. In this study, a large return operation was observed because a simple control waveform was used, but in the future, it will be necessary to design circuits to accommodate multiple operating modes and complex control waveforms, and to design electromagnets capable of generating small-current, large-electromagnetic forces.

Figure 12 shows the planar displacement of a conventional inchworm with wiring and the proposed wireless inchworm during 60 cycles of operation. In the conventional method, the movement trajectory is shifted from a certain point. The movement trajectory after the deviation also extends in a straight line, and it is thought that the movement is restricted by the wiring tension. In contrast, the wireless inchworm moves straight ahead throughout, and the wireless inchworm is believed to have an advantage in wide-range operation. However, with the control method presented in this paper, a significant return motion can be seen in both the conventional and the proposed inchworms from Figure 11. The reason for the return motion is the insufficient holding force of the electromagnets. In addition, the displacement of the wireless inchworm is the same for each cycle, whereas the amount of displacement of the conventional inchworm varies with time.

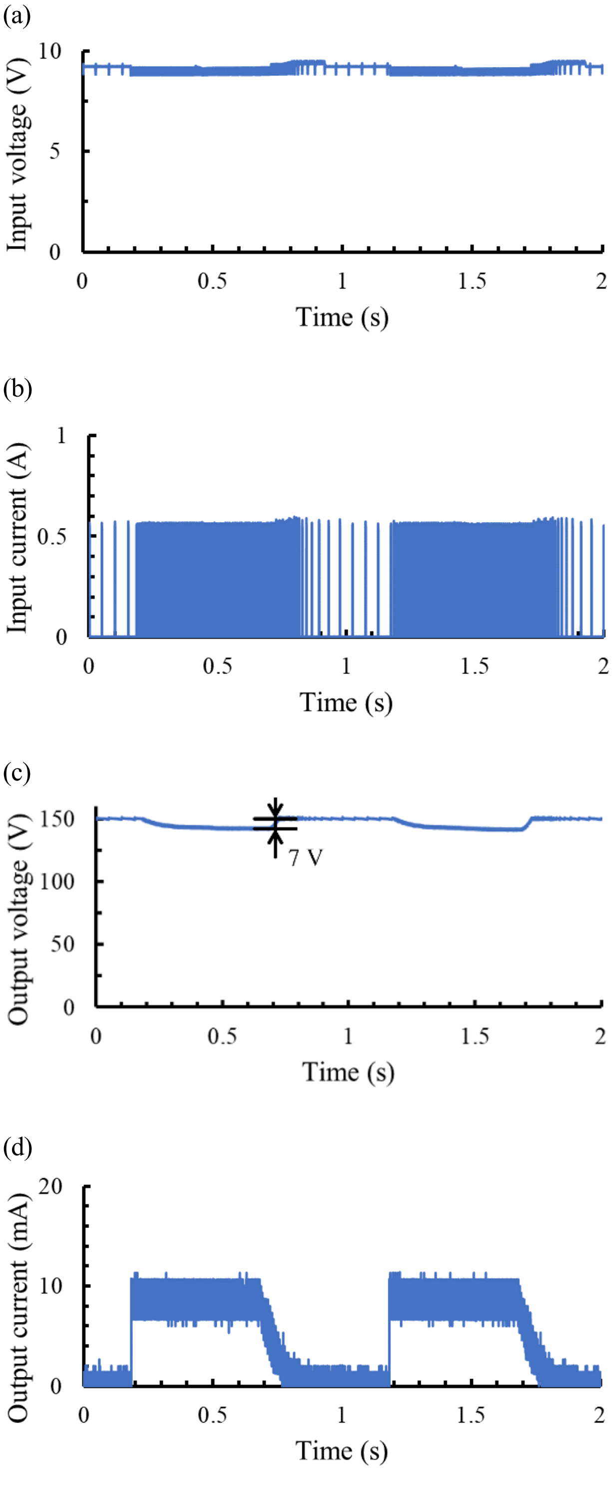

Figure 9. Input/output characteristic of tapped-inductor boost converter while wireless inchworm moves: (a) input voltage; (b) input current; (c) output voltage; and (d) output current.

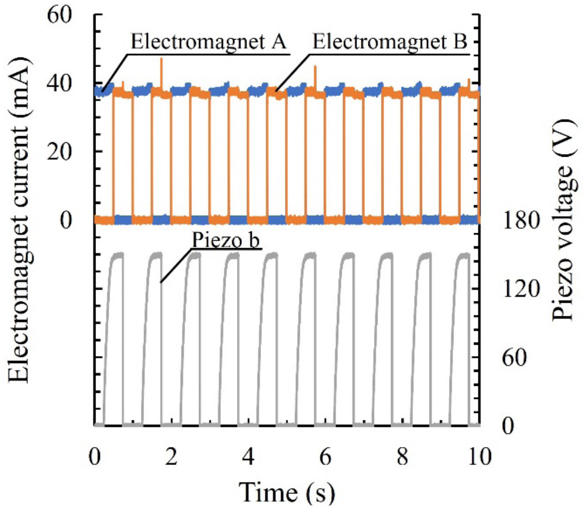

Figure 10. Electromagnet currents and piezo voltage while wireless inchworm moves.

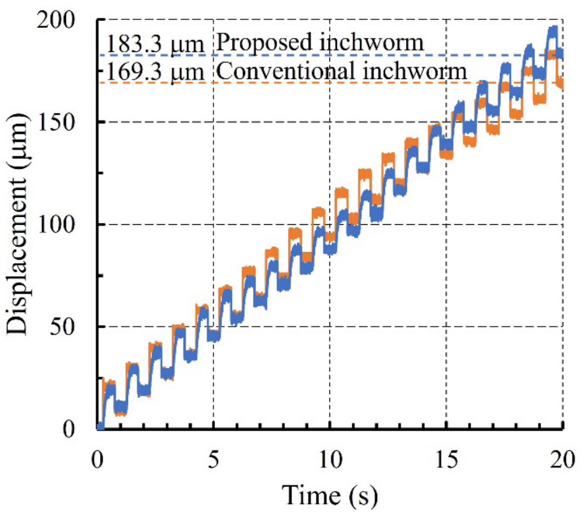

Figure 11. Displacement of wireless inchworm and conventional inchworm.

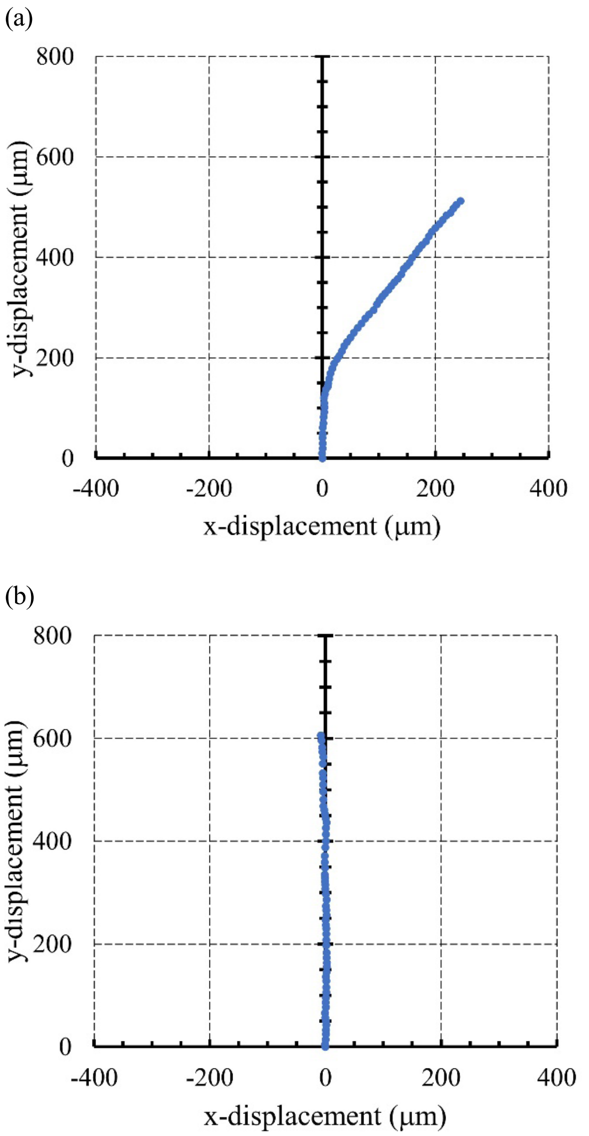

Figure 12. Planar displacement of (a) conventional wiring inchworm; and (b) wireless inchworm.

5. Summary

This paper describes the prototype of a wireless inchworm equipped with a small battery and a tapped-inductor converter. A voltage boost DC/DC converter circuit is installed on the inchworm. The wireless inchworm eliminated the effects of wiring tension caused by power supply cables. A tapped inductor was used to achieve a high boost ratio. The developed DC/DC converter boosted the voltage by 9 V to 150 V, which was suitable for the drive of the piezoelectric actuators. The experimental result shows that the wireless inchworm realised a 9.17 μm incremental linear displacement. The effect of wiring tension on its operation, which has been an issue for inchworms, was reduced, and the limitation of the operating range due to wiring was eliminated. In the future, the displacement of the inchworm will be controlled by tuning the voltage applied to the piezoelectric actuators. The rotational displacement of the wireless inchworm is realised. The communication between the inchworm and the outside environment is also investigated.

Acknowledgements

The financial support from the Japan Society for the Promotion of Science, Grant-in-Aid for Scientific Research (C), No. 21K03972 is acknowledged.

Notes on contributors

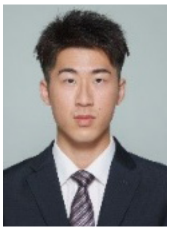

Mr Hayata Takashima graduated from the Aichi Institute of Technology, Japan in 2022 and received his master's degree in electrical and electronics engineering from the Graduate School of Engineering, Aichi Institute of Technology, Japan in 2024. He focused on a microrobot utilising piezoelectric actuators during his graduate research. His special interests included power supply, position measurement, communication, and control strategy of microrobots. He is a member of the Institute of Electrical Engineering of Japan (IEEJ), American Society for Precision Engineering (ASPE), the European Society for Precision Engineering and Nanotechnology (euspen), and the Japan Society for Precision Engineering (JSPE).

Prof Akihiro Torii received his B.S., M.S., and Ph.D. degrees in Electromechanical Engineering from Nagoya University, Japan in 1989, 1991, and 1994, respectively. He is currently a professor with the Faculty of Engineering, Aichi Institute of Technology, Japan. In the period 2002-2003, he was a visiting fellow with the University of Warwick, UK. His research interests include power electronics, micromechatronics, and precision engineering. He is a member of the Institute of Electrical and Electronics Engineers (IEEE), the Institute of Electrical Engineering of Japan (IEEJ), the European Society for Precision Engineering and Nanotechnology (euspen), the Japan Society for Precision Engineering (JSPE), and the Japan Society of Applied-Electromagnetics and Mechanics (JSAEM).

Prof Kae Doki received her B.S., M.S., and Ph.D. degrees from Nagoya University, Japan, in 1997, 1999, and 2002, respectively. She is currently a professor with the Faculty of Engineering, Aichi Institute of Technology, Japan. Her research interests include robotics, man-machine interfaces, human action modelling, and localisation and motion planning of autonomous mobile robots. She is a member of the Institute of Electrical and Electronics Engineers (IEEE), the Institute of Electrical Engineering of Japan (IEEJ), the Robotics Society of Japan (RSJ), and the Society of Instrument and Control Engineering (SICE).

Prof Suguru Mototani received his B.S., M.S., and Ph.D. degrees from Aichi Institute of Technology, Japan in 2004, 2006, and 2009, respectively. After five years' experience in industry, he is currently an associate professor with the Faculty of Engineering, Aichi Institute of Technology. His research interests include wireless power transfer (WPT), especially in special environmental conditions and the topology of WPT electrical circuits. He is a member of the Institute of Electrical Engineering of Japan (IEEJ) and Institute of Electronics, Information and Communication Engineering (IEICE).

References

[1] Bentouati L, Cheknane A, Benyoucef B, and Barambones O (2021). An improved DC-DC converter with high voltage gain based on fully tapped quadratic boost converter for grid connected solar PV micro-inverter. *Transactions of the Institute of Measurement and Control*, 43(1), pp.47-58.

[2] Bez F, Bonanno G, Corradini L, and Garbossa C (2018). Control Technique for Reliable Operation of the Synchronous Series Capacitor Tapped Inductor Converter. *IEEE Transactions on Power Electronics*, 34(8), pp.8150-8161.

[3] Hua S, Liu G, Wang X, Wang Y, and Li J (2014). A Piezoelectric Inchworm Actuator with Bidirectional Thrust Force. *Sensors and Transducers*, 171(5), pp. 169-175.

[4] Kuroda G, Mototani S, Doki K, and Torii A (2021), Stabilization of Power Receiving Coil Voltage by Feedback on Wireless Power Transfer to Small Mobile Robot. *Journal of the Japan Society of Applied Electromagnetics and Mechanics*, 29(1), pp.7-12. (in Japanese).

[5] Liu Y, Sekiguchi R, and Sano Y (2018). Study on Improving Precision of Analysis of Boost Ratio and Power Efficiency of Tapped-Inductor DC-DC Converter Circuit. *Electrical Engineering in Japan*, 202(4), pp. 687-700.

[6] Ma J, Li J, Lin X, He X, Hu Y, Li J, and Wen J (2023). An Inchworm and Stick-Slip Dual Mode Piezoelectric Linear Actuator for Cell Injection. *IEEE Access*, 11, pp. 70534-70541.

[7] Ma X, Liu Y, Deng J, Zhang S, and Liu J (2022). A walker-pusher inchworm actuator driven by two piezoelectric stacks. *Mechanical Systems and Signal Processing*, 169, pp.108636.

[8] Montes JO and Olleros FX (2020). Microfactories and the new economies of scale and scope. *Journal of Manufacturing Technology Management*, 31(1), pp. 72-90.

[9] Okazaki Y, Mishima N, and Ashida K (2004). Microfactory-Concept, History, and Developments. *Journal of Manufacturing Science and Engineering*, 126(4), pp.837-844.

[10] Okazaki Y (2010). Microfactories-A New Methodology for Sustainable Manufacturing. *International Journal of Automation Technology*, 4(2), pp.82-87.

[11] Otake S, Mototani S, Doki K, and Torii A (2021). Design of LC for Wireless Power Transfer ATAC Method to Small Mobile Robot. *Journal of the Japan Society of Applied Electromagnetics and Mechanics*, 30(2), pp. 238-244. (in Japanese).

[12] Poddar SR (2021). Analysis and Design of a Tapped Inductor Boost Converter for a High Voltage Gain Application. *MSE Thesis at the Univ. of Texas at Austin*.

[13] Si ZH, Cheng KW, and Ho SL (2014). Static Performance and Parasitic Analysis of Tapped-inductor Converters. *IET Power Electronics*, 7(2), pp. 366-375.

[14] Sun H, Shi Y, Wang Q, Li X, and Wang J (2022). Modeling and Design Optimization of a New Piezoelectric Inchworm Actuator with Screw Clamping Mechanisms. *Micromachines*, 13(12), pp.2038.

[15] Smith RD, Kolb T, Tanaka S, Lee AK, Harris T, and Barbic M (2022). Robotic multi-probe single-actuator inchworm neural Microdrive. *eLife*, 11, pp.e71876.

[16] Tanabe K, Shiota M, Kusui E, Iida Y, Kusama H, Kinoshita R, Tsukui Y, Minegishi R, Sunohara Y, and Huchiwaki O (2023). Precise Position Control of Holonomic Inchworm Robot Using Four Optical Encoders. *Micromachines*, 14(2), pp. 375.

[17] Torii A, Banno M, Ueda A, and Doki K (2012). A Small-size Self-propelled Stewart Platform. *Electrical Engineering in Japan*, 181(2), pp. 37-46.

[18] Torii A, Mitsuyoshi Y, Mototani S, and Doki K (2018). Orientation Compensation of an Inchworm Stage with Optical Navigation. *International Journal of Automation Technology*, 12(5), pp. 784-790.

[19] Wang S, Rong W, Wang L, Pei Z, and Sun L (2018). A novel inchworm type piezoelectric rotary actuator with large output torque: Design, analysis and experimental performance. *Precision Engineering*, 51, pp.545-551.

[20] Wang J, Huang Hu, Zhang S, Qin Feng, Wang Z, Liang L (2020). Development and analysis of a stick-slip rotary piezoelectric positioner achieving high velocity with compact structure. *Mechanical Systems and Signal Processing*, 145, pp.106895.